JCTC Journal of Chemical Theory and Computation

Article

pubs.acs.org/JCTC

Quantification of Solvent Contribution to the Stability of Noncovalent Complexes

Haiyang Zhang,[†,‡] Tianwei Tan,[†] Csaba Hetényi,[§] and David van der Spoel[‡,*]

[†]Beijing Key Laboratory of Bioprocess, Department of Biochemical Engineering, Beijing University of Chemical Technology, Box 53, 100029 Beijing, China

[‡]Science for Life Laboratory, Department of Cell and Molecular Biology, Uppsala University, Husargatan 3, Box 596, SE-751 24 Uppsala, Sweden

[§]Molecular Biophysics Research Group, Hungarian Academy of Sciences, Pázmány sétány 1/C, H-1117 Budapest, Hungary

Supporting Information

ABSTRACT: We introduce an indirect approach to estimate the solvation contributions to the thermodynamics of noncovalent complex formation through molecular dynamics simulation. This estimation is demonstrated by potential of mean force and entropy calculations on the binding process between β-cyclodextrin (host) and four drug molecules puerarin, daidzin, daidzein, and nabumetone (guest) in explicit water, followed by a stepwise extraction of individual enthalpy (ΔH) and entropy (ΔS) terms from the total free energy. Detailed analysis on the energetics of the host−guest complexation demonstrates that flexibility of the binding partners and solvation-related ΔH and ΔS need to be included explicitly for accurate estimation of the binding thermodynamics. From this, and our previous work on the solvent dependency of binding energies (Zhang et al. *J. Phys. Chem. B* **2012**, *116*, 12684−12693), it follows that calculations neglecting host or guest flexibility, or those employing implicit solvent, will not be able to systematically predict binding free energies. The approach presented here can be readily adopted for obtaining a deeper understanding of the mechanisms governing noncovalent associations in solution.

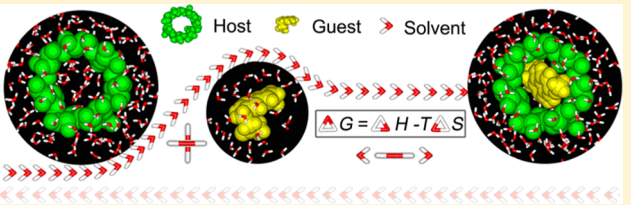

INTRODUCTION

Correct estimation of thermodynamic parameters governing supra-molecular complexation from empirical calculations is of crucial importance for a better understanding of processes in biomolecules and for virtual screening in structure−function analysis and molecular design. For a host−guest complex both enthalpic and entropic contributions from the binding partners and their environment determine the overall binding free energy. Solvent acts not solely as an inert, bulk medium but also as an active partner during the noncovalent complexation. Various methods have been published to evaluate binding free energy profiles, such as molecular mechanics−Poisson−Boltzmann surface area (MM−PBSA),[1] thermodynamic integration (TI),[2] free energy perturbation (FEP),[3] and potential of mean force (PMF) calculations.[4] However, evaluation of solvation enthalpy as well as configurational entropy contributions still remains a challenge, in particular for large biomolecules. Simplified treatments, such as using implicit solvent models based on, for example, atomic fragmental volumes and solvation parameters[5] or treating the receptor as a rigid body in whole or in part, have been proposed to enable high-throughput virtual screening with the aid of docking techniques.[6,7] Efforts to improve the accuracy of scoring functions by including the effects of solvation and receptor flexibility continue as well.[8]

Cyclodextrins (CDs) are ideal candidates for host (or target) molecules, and they have attracted much attention over the years, particularly because of their pharmaceutical applications in drug delivery.[9] The lipophilic cavity and hydrophilic surface of CDs also provide an enzyme-like environment allowing to mimic protein−ligand interactions.[10] Between natural CDs and guest molecules van der Waals, hydrophobic, and hydrogen bond interactions are major driving forces responsible for the host−guest complexation.[11] Release of strain energy in the CD macrocycle and of "high-energy" (also known as enthalpy-rich) water from the CD cavity upon complexation has been suggested to contribute to the binding as well.[12,13] Induced conformational changes of CDs upon binding to a guest have been proposed and detected by experimental and theoretical studies.[14−19] Inoue et al. reported a compensatory enthalpy−entropy relationship in [CD:guest] complexes, based on thermodynamic measurements of CDs with a series of guest molecules via calorimetric titration.[20,21] They stated that steric hindrance in the complex formation may lead to an entropy loss and cancel out the enthalpy gain in part.[21] These observations indicate that solvation-related changes such as desolvation and/or configurational fit play a role in [CD:guest] associations and must be taken into account during calculation of the complexation thermodynamics. Although a number of studies involving free energy calculations of CD-containing

Received: May 16, 2013

   dx.doi.org/10.1021/ct400404q | J. Chem. Theory Comput. XXXX, XXX, XXX−XXX

complexes have been published,[22−27] few reports focus on the solvation problem mentioned above.

Here, we introduce an indirect approach for quantification of solvent contribution to the energetics of noncovalent complexation by molecular dynamics (MD) simulation. This approach is demonstrated on the complex formation between β-CD and four drug molecules (puerarin, daidzin, daidzein, and nabumetone) as host and guest molecules, respectively, using water as explicit solvent. These four drug molecules have been reported to possess potential medicinal values.[28−30] Steered molecular dynamics (SMD)[31] was used to generate a formation process of the [CD:guest] complex, along which potentials of mean force (PMFs, i.e., free energy profiles) were computed with umbrella sampling.[32] More details on the SMD and PMF techniques are given in refs 24, 31, and 33−37. On the basis of PMF calculations, the total enthalpy and entropy change are evaluated and further decomposed into individual items in order to quantify the energetics of binding in detail. The results assist in understanding thermodynamic properties of biological processes such as drug encapsulation and release from CDs. Implications for prediction of receptor−ligand binding affinities in general are discussed at the end of this paper.

METHODS

Simulation Setup. The initial coordinates of the β-CD (host) were extracted from the RCSB protein data bank (PDB code: 1DMB). Drug molecules of puerarin, daidzin, daidzein, and nabumetone (guests) were constructed using the Chem3D software. Structures of the host and guest molecules are shown in Figure 1. The q4md-CD force field was used to model β-CD; this force field has been validated for CD-based systems[38] and for use[39] in the GROMACS suite.[40,41] The generalized Amber force field (GAFF)[42] was chosen to parametrize the guest molecules. Restrained electrostatic potential (RESP)[43] charges of guest molecules were derived by fitting partial charges to electrostatic potentials calculated using Gaussian 03[44] at the HF/6-31G* level of theory. Puerarin, daidzin, and daidzein complexes were simulated at 300 K and nabumetone at 293 K to allow direct comparison with experimental data. Constraints were applied for bond lengths of host and guest molecules with the LINCS algorithm,[45] and for bond lengths and angles of water molecules with SETTLE,[46] allowing a time step of 2 fs. All the simulations were performed with the TIP3P water model,[47] using the GROMACS package (version 4.5.5).[40,41] Long-range electrostatic interactions were treated using the particle mesh Eward (PME) approach[48,49] with a switching distance of 1.0 nm. Further details of the simulation protocol have been presented in ref 16.

Each system contained one host, one guest, and approximately 3300 water molecules in a cubic box of $5 \times 5 \times 4$ nm^3. The host molecule was centered in the box with the Z-coordinate of its seven glycosidic oxygen atoms approximately located at $Z = 2$ nm with the cavity axis of β-CD parallel to the Z-axis. The distance between the center of mass (COM) of the B-ring of the guest and that of the seven glycosidic oxygens of β-CD along the Z-axis was defined as the reaction coordinate ξ (Figure 2). The initial (i) and final (f) values of the reaction coordinate were set to $\xi_i = -2$ nm and $\xi_f = 2$ nm, respectively. Prior to each production we performed an equilibration simulation of 200 ps in which the pressure was maintained at 1 bar with the semi-isotropic Parrinello−Rahman barostat,[50] scaling the box in the $X-Y$ plane only but keeping the box size in the Z-direction fixed. During production simulations the box

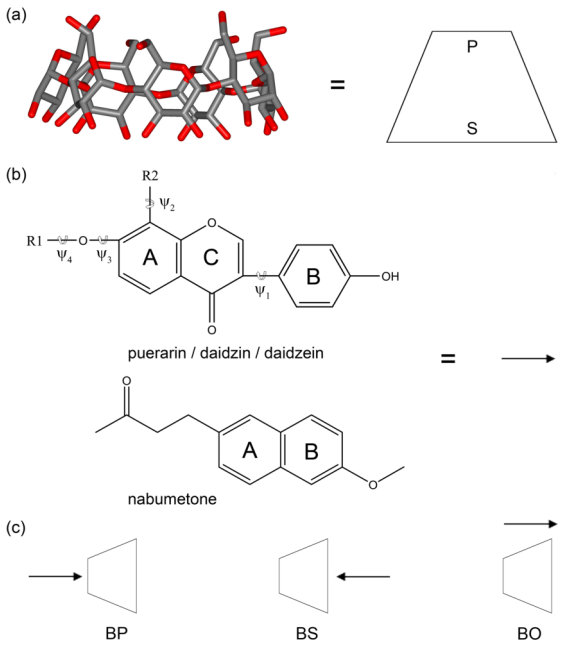

Figure 1. (a) Stick model of β-CD. Hydrogen atoms are omitted for clarity. Primary and secondary hydroxyls are situated at the primary (P) and secondary (S) rim, respectively. (b) Molecular structure of puerarin (R1 = H, R2 = Glucose), daidzin (R1 = Glucose, R2 = H), daidzein (R1 = H, R2 = H), and nabumetone. A, B, and C denote relevant ring groups. Four dihedral angles (ψ_i, i = 1...4) involving non-hydrogen atoms are defined here to describe guest rotations around corresponding bonds. (c) Structural arrangement of the [β-CD:guest] complex formation. BP indicates B-ring of guest inserting into β-CD cavity from the P rim; BS from the S rim. BO means the B-ring locating outside the cavity.

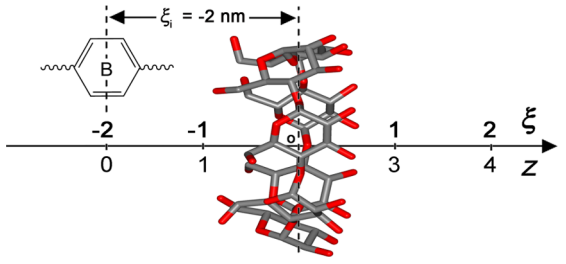

Figure 2. Definition of the reaction coordinate ξ.

size was kept unchanged with no pressure coupling. A periodic pulling simulation was carried out in GROMACS,[40,41] allowing the distance to be larger than half the box size, to obtain a formation event of 1:1 [β-CD:guest] complexes. The seven glycosidic oxygen atoms of β-CD were harmonically restrained with an isotropic force constant of 1000 kJ mol^{-1} nm^{-2} and used as an immobile reference for pulling simulations. The B-ring of the guest was pulled through β-CD cavity from the primary or secondary rim, corresponding to the BP or BS arrangement in Figure 1c, respectively, along the Z-axis over 800 ps with a harmonic force constant of 2000 kJ mol^{-1} nm^{-2} and a pulling rate of 0.005 nm ps^{-1}. In some cases the guest did not go inside but rather outside the cavity, giving a BO arrangement (Figure 1c). The COM distance and reaction coordinate as a function of the simulation time for these three arrangements of [β-CD:puerarin] complexes are shown in Figure S1 in the Supporting Information. Finally the guest sampled 4 nm covering the entire [ξ_i, ξ_f] interval. In the [ξ_i, ξ_f]

dx.doi.org/10.1021/ct400404q | J. Chem. Theory Comput. XXXX, XXX, XXX−XXX

reaction coordinate interval we selected 81 windows with a distance of 0.05 nm between adjacent positions and these windows were then used for umbrella sampling simulations. Following the same scheme, we simulated four guest molecules with three different arrangements and therefore obtained 12 potential of mean force (PMF) profiles in total. In order to detect the ultimate entropy loss of a guest inside a rigid cavity, one more PMF for the [β-CD:nabumetone] complex with the BS arrangement was computed with position restraints of all the non-hydrogen atoms of β-CD. The total simulation time for a single PMF profile was 810 ns (10 ns for each window).

Thermodynamic Calculation. After removing the first 2 ns for equilibration, we constructed the PMFs with a periodic version of the weighted histogram analysis method (WHAM).[51,52] As noted by Kumar and co-workers,[51] the integrated autocorrelation times of the umbrella windows were incorporated into the WHAM iteration procedure to yield a more accurate estimate for the PMF, in particular for a periodic PMF in nonhomogeneous systems.[52] Statistical uncertainties of the PMFs were estimated using the Bayesian bootstrap of complete histograms.[52] All the PMFs were defined to zero at ξ_i and ξ_f where host−guest interactions vanish, and thus, we can quantify the free energy difference (ΔG) with respect to the separated state of the binding partners.

The simulated system was first equilibrated at 1 bar and then the volume was kept constant, so the enthalpy of the system roughly amounts to its internal energy. The temperature is controlled throughout our simulations and thus the kinetic energy has a constant contribution to the internal energy. The enthalpy change (ΔH) therefore reasonably equals the potential energy difference with respect to a completely separated state between host and guest (eq 1).[37] Note that all

$$\Delta H(\xi) = V(\xi) - V(\xi_i) \quad (1)$$

thermodynamic variables are functions of ξ. For simplicity, we omit this functional dependence in the forthcoming text. The entropy change (ΔS) of the system was then computed by subtracting the ΔH part from ΔG (eq 2).

$$-T\Delta S = \Delta G - \Delta H \quad (2)$$

An enthalpic profile of the system was further decomposed into eight terms (eq 3) where the

$$\Delta H = \Delta H_{host} + \Delta H_{guest} + \Delta H_{host-host} + \Delta H_{guest-guest} + \Delta H_{sol-sol} + \Delta H_{host-guest} + \Delta H_{host-sol} + \Delta H_{guest-sol} \quad (3)$$

first two terms contain bonded interactions (bond angle and dihedral angle) and the rest are intra- and intermolecular nonbonded interactions. The bond stretching terms of host and guest molecules amount to zero since all the bond lengths were constrained during the simulation. For the rigid water model TIP3P,[47] bond lengths and angles are fixed and there are no bonded interactions. The nonbonded interaction energy is defined as the sum of respective Lennard-Jones and Coulomb interactions. Decomposition of electrostatic interactions in the reciprocal space when using the PME approach[48,49] is given in the Supporting Information. Error estimates of enthalpy were calculated using a binning analysis.[53]

The configurational entropies of host and guest molecules were computed from the covariance matrices of their atomic fluctuations using the quasiharmonic approximation.[54] We first calculated entropy changes of host and guest with respect to the unbound state separately and then subtracted them from ΔS to obtain the solvent entropy change involved with, for instance, solvent rearrangements during desolvation of host and guest molecules upon binding (eq 4).

$$\Delta S_{sol} = \Delta S - \Delta S_{host} - \Delta S_{guest} \quad (4)$$

Since the error in ΔH would propagate to ΔS, all entropy terms here were assumed to have the same errors as ΔH.

RESULTS

Complex Arrangement. Potential of mean force (PMF) profiles for the formation process of 1:1 [β-CD:puerarin] complexes with BP, BS, and BO arrangements and representative states (A...G) in the reaction coordinate ξ are presented in Figure 3. The three structural arrangements refer

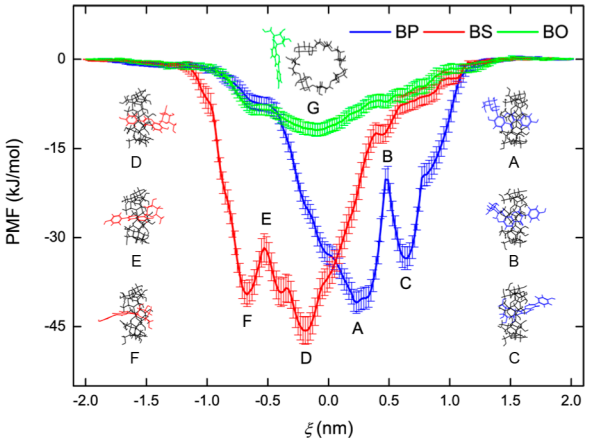

Figure 3. Potential of mean force (PMF) profiles for the [β-CD:puerarin] complex formation in three structural arrangements (BP, BS, and BO). Representative configurations along ξ are shown using line model. β-CD is colored in black and puerarin in the same color as the arrangement.

to Figure 1c. BP and BS in our simulations indicate that the B-ring of guest inserts into CD cavity along the $+\xi$ and $-\xi$ direction, respectively.

As shown in Figure 3, periodic PMFs ensure equality of the guest located at $\xi = -2$ and 2 nm. All the PMFs approach to zero and level off on both sides of the reaction coordinate where there is no interaction between β-CD and puerarin. The A- and D-states with B- and C-rings of puerarin inside the β-CD cavity give the most stable inclusion configuration for BP and BS, respectively. When the A-ring of puerarin approaches the cavity, such as in the B- and E-states, an energy barrier is observed and this barrier might prevent puerarin from further penetrating into the CD cavity. The C- and F-states with the glucose unit of puerarin inside the cavity form local minima in the PMFs. As expected, there is no obvious barrier and a weaker binding is observed for the BO arrangement, as in the G-state, due to a less efficient contact of hydrophobic moieties between host and guest, compared to the inclusion complexes such as BP and BS. For the G-state, puerarin binds to the outer surface of β-CD with its isoflavone skeleton (i.e., the A, B, and C rings in Figure 1b) perpendicular to the glucopyranose residue of β-CD; this way the hydrophobic contact area appears to be maximized. The D-state is more energetically favorable than the A-state and therefore is the most probable

dx.doi.org/10.1021/ct400404q | J. Chem. Theory Comput. XXXX, XXX, XXX−XXX

configuration, in good agreement with the experiment where a very similar [β-CD:puerarin] inclusion complex (such as the D-state) was detected in aqueous solution by NMR spectroscopy.[55]

PMF profiles (ΔG) for puerarin and daidzin are presented in Figure 4. Daidzin behaves similar as puerarin, whereas it can

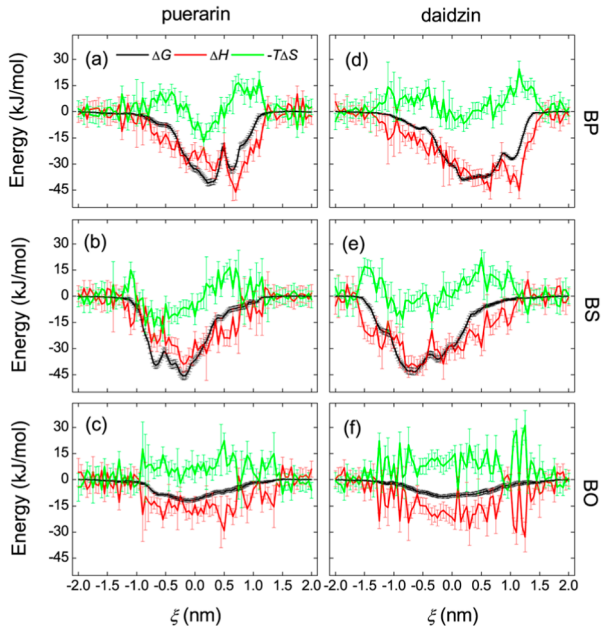

Figure 4. Thermodynamic profiles (ΔG, ΔH, and $-T\Delta S$) of the system for the complex formation of β-CD with puerarin and daidzin in three patterns BP, BS, and BO.

insert into β-CD cavity more deeply than puerarin in the BS arrangement (Figure 4, panels b and e). PMF profiles (ΔG) for daidzein and nabumetone are given in Figure S2 in the Supporting Information. For daidzein and nabumetone no pronounced energy barriers are observed, and both BP and BS are thermodynamically stable although BS is preferred slightly over BP. NMR experiments have identified these two possible [β-CD:nabumetone] inclusion complexes.[56] When hydrophobic moieties of the guest (such as daidzin, daidzein, and nabumetone) stay inside β-CD cavity, the PMF profiles display a flat landscape (Figure 4 and Supporting Information Figure S2), implying that there is almost no energy barrier and the guest can shuttle freely inside the cavity to some extent. A shuttling motion of puerarin and daidzin inside β-CD cavity in the BS pattern has indeed been detected by MD simulations.[57]

System Thermodynamics. Thermodynamic profiles (ΔG, ΔH, and ΔS) of the system along ξ for the four guests with BP, BS, and BO arrangements are shown in Figure 4 and Supporting Information Figure S2. Here entropy is presented as $-T\Delta S$. From these profiles we can derive contributions of enthalpy and entropy to ΔG. A reduced enthalpy (more favorable) is observed for all the guests upon complexation, while entropy increases in some cases and decreases in other. The thermodynamic stability of these complexes can be therefore attributed to a combination of both ΔH and ΔS. As shown in Figure 4a, for instance, both enthalpy and entropy gains favor a stable complex (i.e., the A-state in Figure 3), which corresponds to the global minimum of the PMF. When puerarin enters the β-CD cavity more deeply with its glucose unit inside the cavity (such as the C-state in Figure 3), ΔH reaches a maximum, whereas an entropy loss cancels out this enthalpy gain, giving a moderate ΔG (Figure 4a). Unlike the C-state, the D-state in Figure 3 is a maximum of enthalpy gain and has an entropy gain, forming a global minimum of ΔG (Figure 4b). The other three guest molecules display similar enthalpy–entropy relationships to puerarin for BP and BS (Figure 4 and Supporting Information Figure S2). For BO, enthalpy gain and entropy loss are detected for puerarin and daidzin (Figure 4, panels c and f), whereas for daidzein and nabumetone the complex stability seems to result exclusively from the enthalpy (Supporting Information Figure S2, panels c and f). Interestingly, puerarin, daidzin, and daidzein share the same isoflavone skeleton and have similar enthalpy gains upon binding to the outer surface of β-CD, but an entropy loss decreases the binding of puerarin and daidzin. This entropy loss may be due to the limited movement of the glucose unit when interacting with the β-CD surface. Daidzein does not have such glucose group (Figure 1b), and there is no significant change in entropy, leading to a relatively stronger binding (Supporting Information Figure S2c).

Now, we turn to the standard thermodynamics of the entire binding reactions for [β-CD:guest] associations. A cylinder approximation[22,58−60] was used to evaluate the standard binding free energies. When a guest enters the β-CD cavity, the sampled volume for the guest is restrained to a small cylinder defined by the area accessible for guest movement in the $X-Y$ plane. The average radius of that cylinder, $r(\xi)$, was obtained from COM positions of the guest at each window. The association equilibrium constant K_a is written as

$$K_a = \pi N_A \int r(\xi)^2 \exp[-\Delta G(\xi)/RT]\mathrm{d}\xi \tag{5}$$

where N_A is Avogadro constant and R the ideal gas constant.[58,59] The thermodynamics of binding can therefore be calculated using

$$\Delta G^0 = -RT\ln(K_a C^0) \tag{6}$$

$$\Delta H^0 = RT^2 \frac{d}{dT}\ln(K_a C^0) = \frac{\int r(\xi)^2 \Delta G(\xi) \exp[-\Delta G(\xi)/RT]\mathrm{d}\xi}{\int r(\xi)^2 \exp[-\Delta G(\xi)/RT]\mathrm{d}\xi} \tag{7}$$

$$-T\Delta S^\circ = \Delta G^\circ - \Delta H^\circ \tag{8}$$

where C° is the standard concentration of 1 mol/L.[61] Note that ΔG° here is the standard free energy of the binding process, while $\Delta G(\xi)$ denotes free energy profiles obtained from PMF calculations. The integration is limited to the interval over which host and guest molecules associate. As noted by Bonal and co-workers,[60] the integration was computed from each side of the PMF profile (where host and guest have no interaction) to the central maximum and they averaged over these two reaction pathways to obtain the thermodynamic parameters. A similar treatment is adopted in our calculation to define the integration interval in eqs 6 and 7. For the cases where there is no obvious central maximum in the PMF, such as daidzein (Supporting Information Figure S2a) and nabumetone (Figure S2e), we perform the integral over the whole PMF.

Table 1 lists the calculated ΔG° for the four drugs studied. For daidzein and nabumetone, ΔG° compares well with the experiment, while the calculation overestimates the binding strength between β-CD and puerarin. The results depend on

dx.doi.org/10.1021/ct400404q | J. Chem. Theory Comput. XXXX, XXX, XXX−XXX

Table 1. Comparison of Calculated Binding Free Energy (kJ/mol) with Experimental Determinations

guest	T (K)	$-\Delta G_{exp}$	$-\Delta G^0_{cal}$ BP	$-\Delta G^0_{cal}$ BS
puerarin	300	19.0[a]	26	32
daidzin	300		24	29
daidzein	300	16.6[b]	19	22
nabumetone	293	19.2[c] /19.7[d] /18.7[e]	18	21

[a]Taken from ref 55. [b]Ref 62. [c]Ref 56. [d]Ref 63. [e]Ref 64.

the interval used for integration for sure; a shorter interval gives a weaker binding. If β-CD in the simulation is more rigid that in the experiment, there would exist energy barriers preventing the guest from further accessing some part of the binding site. That is, a more rigid host would lead to a shorter integration interval. If so, we can get much closer to the experiment by adjusting the host flexibility artificially. Another factor responsible for the source of error could probably be the force field used. Data for $\Delta H°$ and $\Delta S°$ are given in Tables S2 and S3 in the Supporting Information. For nabumetone, there is some discrepancy between calculated and observed $\Delta H°$ and $\Delta S°$ (in exp. 2 and 3, but not 1, Table S3).

Enthalpy Decomposition. For a better understanding of the distinct shape of an enthalpic profile, we decomposed it into eight terms including bonded and nonbonded interactions (eq 3). Figure 5 shows the ΔH decomposition for the [β-CD:puerarin] complex formation. For BP and BS, changes in ΔH_{host} and ΔH_{guest} upon binding are positive, which means that the bonded term of binding partners tends to disfavor host−guest inclusion complexations, indicated by black and red lines (Figure 5, panels a and b). For BO (Figure 5c), no significant changes are observed for ΔH_{host} and ΔH_{guest}. $\Delta H_{host-host}$ and $\Delta H_{guest-guest}$ (green and blue lines, panels a and b in Figure 5) tend to favor host−guest complexations (negative values). There are significant enthalpy changes in intramolecular interactions of the host ($\Delta H_{host-host}$) for BP and BS; no obvious changes for BO.

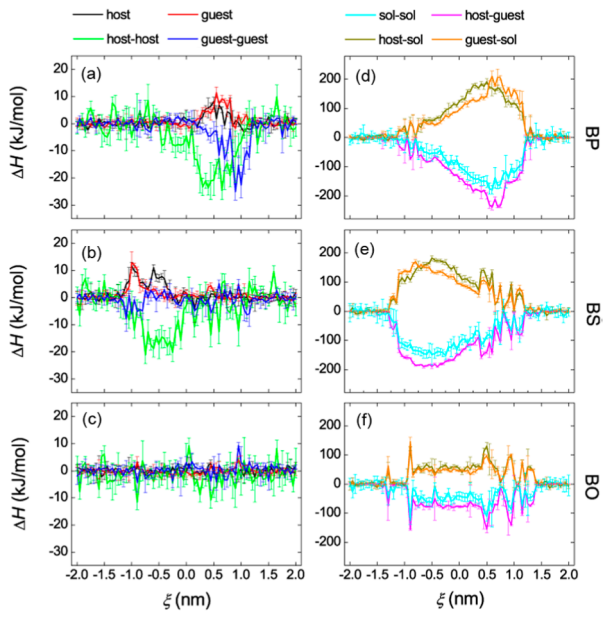

Figure 5. Enthalpy decomposition for the complex formation of β-CD with puerarin in three patterns BP, BS, and BO.

When a guest travels from the bulk into the CD cavity, the solvent molecules entrapped inside the cavity will be expelled, a process such as the release of "high-energy" water. Another contribution to the energetics is due to release of water molecules that participate in host and guest solvation. As a result, the water−water enthalpy $\Delta H_{sol-sol}$ becomes more negative (the cyan line in Figure 5, panels d−f). Unsurprisingly, the strength of the intermolecular interaction between host and guest ($\Delta H_{host-guest}$) increases when forming a complex, as indicated by the magenta line. Accompanied by desolvation, the strength of the interaction between host (or guest) and solvents decreases (positive ΔH, dark yellow and orange lines in Figure 5). When accommodating puerarin as a guest, β-CD reaches a desolvation maximum ($\Delta H_{host-sol}$, panels d and e in Figure 5) where the A- and C-rings of the guest are inserted into the cavity and the glucose unit stays very close to the cavity, such as in the B- and E-states in Figure 3. When the glucose unit of puerarin goes further and stays inside the cavity (C- and F-states in Figure 3), host desolvation gets weakened and guest desolvation maximized (Figure 5, panels d and e). The guest bound to β-CD outer surface also affects (de)solvation of host and guest molecules, but to a lesser degree (Figure 5, panels d−f). Similar observations are detected as well for β-CD complexes with daidzin, daidzein, and nabumetone, as shown in Figures S3−S5, respectively, in the Supporting Information. Since daidzein and nabumetone do not possess a glucose unit, they give more symmetrical profiles of the ΔH decomposition (Figures S4 and S5).

Entropy Decomposition. In order to distinguish individual entropy contributions clearly, the total entropy was decomposed into three single terms corresponding to host, guest, and solvent molecules (eq 4) and presented as $-T\Delta S$. Figure 6 shows the entropy decomposition for β-CD complexes with puerarin and daidzin; data for daidzein and nabumetone are given in Figure S6 in the Supporting Information. An

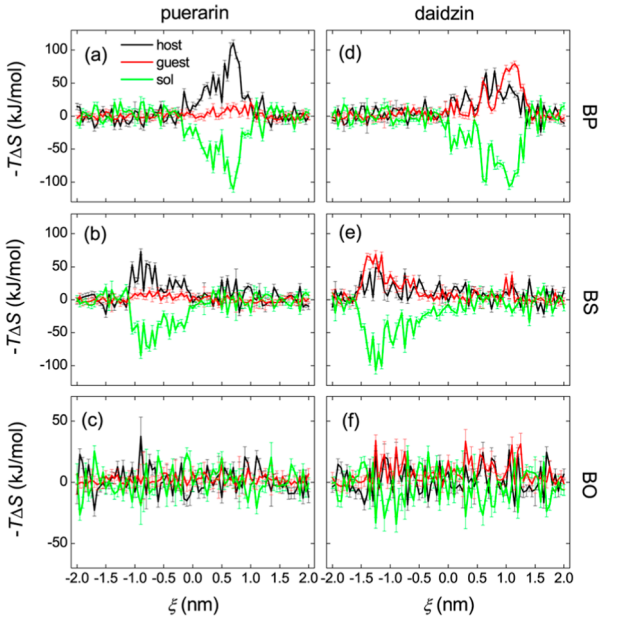

Figure 6. Entropy decomposition for the complex formation of β-CD with puerarin and daidzin in three patterns BP, BS, and BO.

dx.doi.org/10.1021/ct400404q | J. Chem. Theory Comput. XXXX, XXX, XXX−XXX

Table 2. Individual Contribution (kJ/mol) of ΔH and ΔS Weighted by Boltzmann Factors for the Actual Binding Reactions between β-CD and Guest Molecules with BP and BS Arrangements (Standard Deviations in Parentheses)

	puerarin		daidzin		daidzein		nabumetone	
$\langle\Delta E\rangle$	BP	BS	BP	BS	BP	BS	BP	BS
ΔH_{host}	2(1)	1(1)	1(1)	−1(1)	1(1)	1(1)	−1(1)	0(1)
ΔH_{guest}	3(1)	1(1)	0(1)	−1(1)	0(1)	0(1)	0(1)	0(1)
$\Delta H_{host-host}$	−17(3)	−13(3)	−9(2)	−8(2)	−9(2)	−10(3)	−12(3)	−10(2)
$\Delta H_{guest-guest}$	−1(1)	−1(1)	−4(2)	0(1)	0(1)	1(1)	−2(1)	−3(1)
$\Delta H_{sol-sol}$	−136(8)	−130(7)	−123(7)	−123(6)	−98(7)	−106(6)	−96(7)	−111(8)
$\Delta H_{host-guest}$	−176(8)	−170(7)	−163(4)	−164(5)	−129(9)	−128(7)	−123(8)	−126(7)
$\Delta H_{host-sol}$	168(9)	155(8)	142(6)	145(6)	119(7)	119(8)	131(8)	132(8)
$\Delta H_{guest-sol}$	127(7)	123(7)	119(5)	117(5)	86(6)	85(6)	80(6)	85(6)
$-T\Delta S_{host}$	42(4)	24(3)	24(3)	14(3)	14(3)	9(2)	21(3)	18(3)
$-T\Delta S_{guest}$	4(2)	7(2)	13(3)	23(4)	0(1)	0(1)	11(2)	14(2)
$-T\Delta S_{sol}$	−55(4)	−38(4)	−38(3)	−41(4)	−12(3)	−14(3)	−33(5)	−33(4)

obvious entropy loss of the host and a slight loss of the guest are observed for puerarin with BP and BS arrangements (Figure 6, panels a and b). For daidzin there are pronounced entropy losses for both the host and guest (Figure 6, panels d and e), due to loss of flexibility in host and guest molecules upon complexation. For puerarin, daidzin, and nabumetone in BP and BS patterns, the solvent in contrast tends to gain entropy (positive ΔS), favoring the complexation. No obvious changes in ΔS are detected for the [β-CD:daidzein] inclusion (Figure S6, panels a and b). Binding of a guest to the outer surface of β-CD may also result in an entropy change to a certain extent (Figure 6 and Supporting Information Figure S6).

Figure S7 in the Supporting Information presents thermodynamic profiles for the BS [β-CD:nabumetone] inclusion with a flexible or rigid host. Compared to the flexible host, the rigid one gives more minima in the PMF and has a weaker binding to nabumetone due to a less favorable enthalpy gain (Supporting Information, Figure S7, panels a and b), as indicated by the ΔH decomposition (Supporting Information, Figure S7, panels c−f). As expected, the rigid host displays little entropy loss upon binding to the guest since all the non-hydrogen atoms are harmonically fixed. When entrapped inside a rigid cavity, nabumetone shows larger entropy loss and solvent molecules give a larger entropy gain (Supporting Information, Figure S7, panels g and h).

For a quantitative determination of the energetics, individual contributions of $\Delta H(\xi)$ and $-T\Delta S(\xi)$ are weighted by their Boltzmann factors (eq 9)

$$\langle\Delta E\rangle = \frac{\int \Delta E(\xi)\exp[-\Delta G(\xi)/RT]\mathrm{d}\xi}{\int \exp[-\Delta G(\xi)/RT]\mathrm{d}\xi} \quad (9)$$

where ΔE represents ΔH or $-T\Delta S$. Weighted values for the actual binding reactions are tabulated in Table 2, showing similar observations to what was mentioned above.

Guest Rotation. The configurational entropy here was determined from covariance matrices of atomic fluctuations.[54] A guest entrapped inside the CD cavity probably cannot rotate as freely as it is in the bulk, which may limit structural fluctuations of the guest and hence cause an entropy loss. To detect guest rotations in the free and complex state, four dihedral angles were defined in Figure 1b. Dihedral potentials of the four angles taken from the GAFF parameters[42] are given in Figure S8 in the Supporting Information. A large energy barrier exists for ψ_1, meaning that it is not easy for ψ_1 to rotate. There are smaller barriers for ψ_3 and ψ_4; no barrier for ψ_2. It should be noted that Supporting Information Figure S8 shows the intrinsic barrier only and dihedral rotations also depend on the environment of the molecule.

Distributions of these dihedrals (ψ_i, i = 1...4) during the formation process of β-CD with puerarin and daidzin in the BP pattern are presented in Figure 7. Free states for puerarin and daidzin locate at ξ = −2.0 nm. The B-ring of guest inserted into β-CD cavity at ξ = 0.5 nm; the glucose unit of guest stays inside the cavity at ξ = 1.0 nm. For puerarin and daidzin in the free and complex state, there is no significant difference for ψ_1, and the same goes for daidzein (not shown here). The glucose rotation (ψ_2) for puerarin is almost not affected when entrapped inside the cavity, and it is similar to the free state, which may explain the small entropy change of guest in Figure 6a. Hydrogen-bonding interactions between the hydroxyl group connected to A-ring and the glucose unit of puerarin are

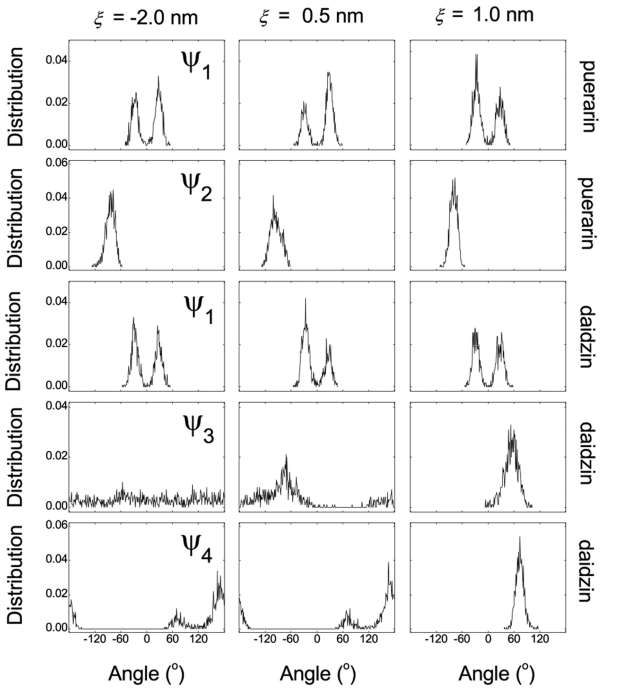

Figure 7. Distribution of dihedral angles for puerarin (ψ_1 and ψ_2) and daidzin (ψ_1, ψ_3, and ψ_4) with the BP arrangement along ξ. Dihedral distribution for daidzein (ψ_1) is similar to that for puerarin and daidzin.

dx.doi.org/10.1021/ct400404q | J. Chem. Theory Comput. XXXX, XXX, XXX−XXX

observed in the simulation, which may limit the rotation of ψ_2. For daidzin, the glucose unit rotates freely in the free state (ξ = −2.0 nm), as indicated by ψ_3 and ψ_4, whereas their rotations are evidently limited when the glucose unit stays inside the cavity at ξ = 1.0 nm (Figure 7). This finding explains the large entropy loss of daidzin upon binding to β-CD in Figure 6d.

DISCUSSION

When typical cyclodextrins (α-, β-, and γ-CD containing six, seven, and eight glucopyranose residues in a ring, respectively) form 1:1 complexes with asymmetrical guest molecules, three possible arrangements (BP, BS, and BO in Figure 1c) may be adopted and they are expected to be different in energy due to the guest orientation. Much attention has been paid to BP and BS inclusion patterns both in academic research and industrial applications, since the CD cavity is a specific binding site and the outer surface is not. The asymmetric free energy profiles for the BP and BS arrangements in our simulations (Figures 3 and 4) indicate the difference in the specific binding and in two types of inclusion complexes. Many compounds have been reported to show two possible inclusion models with CDs, such as surfactants with typical CDs[18,65] and steroid drugs,[22] flavanols,[66,67] and aziadamantane derivatives[68] with β-CD.

Host−guest complexes are often used as models to gain general insights on the thermodynamics of binding, due to their small size and simplicity compared to protein−ligand systems. Many projects have been devoted to studying the thermodynamics of cyclodextrin complexation using PMF calculations.[39,60,69−72] Cai and co-workers reported a decomposition of the PMF profile into van der Waals (host−guest), electrostatic (host−guest), and host−solvent interactions.[69−71] In addition, Kovalenko et al. proposed a spatial decomposition analysis for the cyclodextrin complexation and decomposed the thermodynamics into the excluded volume and solvation shell terms.[73] In a very recent study, Wickstrom et al. indicated that the binding free energy can be decomposed into the reorganization free energy and the average binding energy.[74] In this work, we introduce another decomposition to characterize the total and individual contributions (ΔH and ΔS) from the binding partners as well as their solvation environment, as described in detail in the Methods section.

Thermodynamic profiles of the system (Figure 4 and Supporting Information Figure S2) show that both enthalpy and entropy contribute to the binding between the model host β-CD and the guests studied. Such binding reactions are predominantly enthalpy-driven and in some cases an entropy loss weakens the binding. Decomposition of the total enthalpy (ΔH) provides more information on individual contributions from intra- and intermolecular interactions, as shown in Figure 5 and Supporting Information Figures S3−S5. As expected, desolvation of host and guest molecules gives an unfavorable ΔH and the complex formation produces a favorable ΔH. The solvent favors the complex stability as well with enthalpy gains. Surprisingly, the numerical values of these four terms ($\Delta H_{host-sol}$, $\Delta H_{guest-sol}$, $\Delta H_{host-guest}$, and $\Delta H_{sol-sol}$) are an order of magnitude larger than that for the thermodynamic parameters of the entire binding reactions, as shown in Tables 1 and 2 and Supporting Information Tables S2−S3, which implies that these contributions to the binding need to be considered with care. Moreover, changes in intramolecular energies of the binding partners (ΔH_{host}, ΔH_{guest}, $\Delta H_{host-host}$, and $\Delta H_{guest-guest}$), in particular for nonbonded interactions of the host ($\Delta H_{host-host}$), indicate that host molecules adjust their configurations to the binding environment, and so do guest molecules. This adjustment (configurational fit) reflects fluctuations in atomic positions, known as guest-induced effects,[14] leading to changes in the potential energy and thus to ΔH between 8 and 17 kJ/mol. Dolenc et al. investigated the effect of receptor flexibility on the binding affinity and reported that neglecting the receptor flexibility affected the model structures of the complex and enthalpy contributions to the binding, in particular for a flexible receptor such as DNA.[23] Since the contributions from conformational changes are on the same order of magnitude as the standard thermodynamics of binding (Tables 1 and 2 and Supporting Infomation Tables S2−S3), these need to be considered explicitly when computing binding energies.

For the entropy (ΔS) decomposition in Figure 6, most of entropy changes take place when flexible moieties of the guest are included inside the CD cavity or interact with the CD surface. Both host and guest may lose entropy upon binding, depending on the guest and orientation. The solvent, however, tends to have an entropy gain, favoring the complex formation. Desolvation of the binding partners liberates solvent molecules participating in the solvation, allowing a greater degree of freedom for motion of these water molecules and hence increased entropy, in line with common perception of the hydrophobic effect.[75,76] Daidzein, the most hydrophobic and rigid molecule among the tested guests, has weaker interactions with water molecules and undergoes smaller fluctuations in structure. Inclusion of daidzein to the CD cavity should perturb the binding-site waters and displace them from the cavity. For the solvent, this process ought to give favorable ΔS. However, no significant ΔS for β-CD, daidzein, and water molecules is observed upon complexation in the simulation (Supporting Information Figure S6). This finding could be ascribed to the fact that rigidity of daidzein leads to a weaker (de)solvation and does not affect the surrounding environment too much.

As ideal host−guest models, the [CD:drug] complexes studied in this work hold valuable implications for the receptor−ligand binding. It has been realized for a long time that for truly predictive estimates of ligand−binding energies free energy methods are crucial.[77] However the (high-throughput) virtual screening concept has remained popular, despite suggestions that it may not live up to the hype.[78] Docking and binding-site predictions can yield good candidates for binding sites,[79] but the built-in scoring functions are not necessarily predictive of binding strength,[80] and docking codes are therefore regarded with some skepticism.[81] For high-throughput virtual screening to work, an accurate estimation of the contribution from solvation and from conformational changes would be needed, without the computational cost associated with free energy calculations. Based on our calculations, changes in intramolecular interactions due to configurational fit contribute significantly to the complexation thermodynamics (Figure 5 and Supporting Information Figures S3−S5). Moreover, we observe a large enthalpy gain of the solvent environment for both flexible and rigid hosts, and this contribution most likely cannot be evaluated accurately when neglecting the solvent or using implicit solvent.

Entropy estimation, especially for the solvent environment, is another difficulty faced by high-throughput virtual screening. A detailed review for theory of free energy and entropy in noncovalent binding has been presented by Zhou and Gilson.[82] In this work, we used a quasiharmonic approximation[54] to calculate the configurational entropy; the Schlitter formula was

dx.doi.org/10.1021/ct400404q | J. Chem. Theory Comput. XXXX, XXX, XXX−XXX

also tested.[83] We note that the quasiharmonic method is an approximation, which does not approach the true entropy even in the limit of infinite sampling, but these two methods were reported to be useful for ΔS estimation of ligands in binding processes.[84] For our cases, the two methods yield very similar results for the relative ΔS (which is very important in this analysis presented), although the absolute values differ (not shown here). The entropy of the host and guest can be computed readily, and this has been incorporated in methods for estimating the binding energy of complexes.[6,7,85] In our calculations, the solvent entropy is computed indirectly using eq 4, and its accuracy depends on the estimation of ΔG and ΔH and the values of $-T\Delta S$ depend heavily on the guest, varying between −12 to −55 kJ/mol (Table 2). The results show that the solvent tends to gain entropy and cancel out most of the entropy losses of the binding partners. Neglecting either of the flexibility or the entropy items would yield an error with the same order of magnitude as the entire binding energy. It is therefore difficult to imagine that the accuracy of scoring functions for use in virtual screening (e.g., pharmaceutical design and biotechnology projects) can be increased sufficiently to systematically reach an accuracy comparable to free energy calculations.[77]

CONCLUSION

In this work, all possible complex arrangements between a model host (β-CD) and four drug guests (puerarin, daidzin, daidzein, and nabumetone) were evaluated through steered molecular dynamics and potential of mean force calculations. The total and individual contribution of enthalpy and entropy to the stability of such noncovalent complexes were analyzed in terms of binding mode, solvation, and structural flexibility. Our results show that host flexibility, solvent enthalpy, and solvent entropy play important roles in host−guest complexation, and these items need to be included explicitly for accurate calculation of the binding thermodynamics. We have previously demonstrated that the binding energy of [host:guest] complexes in different organic solvents is only weakly correlated to solvent properties such as the dielectric constants or Log P.[39] An implicit solvent model can provide a useful estimate of solvation free energy only if used under the conditions it was parametrized for (temperature, solvent) and if there are no very specific hydrogen bonds. Implicit models are not suitable to provide detailed information on how that free energy is partitioned into enthalpy and entropy. Full molecular dynamics (MD) simulations using explicit solvents are therefore required for precise estimation of thermodynamic parameters of molecular complexation.

ASSOCIATED CONTENT

Supporting Information

Decomposition of reciprocal Ewald sum (Table S1), calculated $\Delta H°$ and $\Delta S°$ (Tables S2 and S3), COM pulling for puerarin (Figure S1), thermodynamic profiles of the system for daidzein and nabumetone (Figure S2), ΔH decomposition for daidzin, daidzein, and nabumetone (Figure S3−S5), ΔS decomposition for daidzein and nabumetone (Figure S6), thermodynamic profiles for nabumetone with a flexible or rigid host (Figure S7), and dihedral potential (Figure S8). This material is available free of charge via the Internet at http://pubs.acs.org.

AUTHOR INFORMATION

Corresponding Author

*E-mail: spoel@xray.bmc.uu.se.

Notes

The authors declare no competing financial interest.

ACKNOWLEDGMENTS

We thank Dr. Daniel Larsson and Dr. Jochen Hub for assistance. The Swedish research council is acknowledged for a grant of computer time (SNIC020-11-15) through HPC2N. H.Z. thanks the China scholarship council for support. This work was supported by the National Basic Research Program of China (973 program: 2013CB733600, 2012CB725200, and 2011CB710800), the National Nature Science Foundation of China (21106005, 21076017, and 21306006), and National High-Tech R&D Program of China (863 program: 2012AA022205D, 2012AA021404, and 2011AA02A205).

REFERENCES

(1) Srinivasan, J.; Cheatham, T. E.; Cieplak, P.; Kollman, P. A.; Case, D. A. Continuum Solvent Studies of the Stability of DNA, RNA, and Phosphoramidate−DNA Helices. *J. Am. Chem. Soc.* **1998**, *120*, 9401−9409.

(2) Straatsma, T. P.; Berendsen, H. J. C. Free Energy of Ionic Hydration: Analysis of a Thermodynamic Integration Technique to Evaluate Free Energy Differences by Molecular Dynamics Simulations. *J. Chem. Phys.* **1988**, *89*, 5876−5886.

(3) Pearlman, D. A.; Kollman, P. A. A New Method for Carrying out Free Energy Perturbation Calculations: Dynamically Modified Windows. *J. Chem. Phys.* **1989**, *90*, 2460−2470.

(4) Kirkwood, J. G. Statistical Mechanics of Fluid Mixtures. *J. Chem. Phys.* **1935**, *3*, 300−313.

(5) Stouten, P. F. W.; Frömmel, C.; Nakamura, H.; Sander, C. An Effective Solvation Term Based on Atomic Occupancies for Use in Protein Simulations. *Mol. Simulat.* **1993**, *10*, 97−120.

(6) Lang, P. T.; Brozell, S. R.; Mukherjee, S.; Pettersen, E. F.; Meng, E. C.; Thomas, V.; Rizzo, R. C.; Case, D. A.; James, T. L.; Kuntz, I. D. Dock 6: Combining Techniques to Model RNA−Small Molecule Complexes. *RNA* **2009**, *15*, 1219−1230.

(7) Morris, G. M.; Huey, R.; Lindstrom, W.; Sanner, M. F.; Belew, R. K.; Goodsell, D. S.; Olson, A. J. Autodock4 and Autodocktools4: Automated Docking with Selective Receptor Flexibility. *J. Comput. Chem.* **2009**, *30*, 2785−2791.

(8) Gohlke, H., Ed. Protein−Ligand Interactions. In *Methods and Principles in Medicinal Chemistry*; Mannhold, R.; Kubinyi, H.; Folkers, G., Eds. Wiley-VCH: Weinheim, 2012; Vol. *53*.

(9) van de Manakker, F.; Vermonden, T.; van Nostrum, C. F.; Hennink, W. E. Cyclodextrin-Based Polymeric Materials: Synthesis, Properties, and Pharmaceutical/Biomedical Applications. *Biomacromolecules* **2009**, *10*, 3157−3175.

(10) Fan, Z.; Diao, C.-H.; Song, H.-B.; Jing, Z.-L.; Yu, M.; Chen, X.; Guo, M.-J. Encapsulation of Quinine by β-Cyclodextrin: Excellent Model for Mimicking Enzyme−Substrate Interactions. *J. Org. Chem.* **2006**, *71*, 1244−1246.

(11) Shin, K.-m.; Dong, T.; He, Y.; Taguchi, Y.; Oishi, A.; Nishida, H.; Inoue, Y. Inclusion Complex Formation between α-Cyclodextrin and Biodegradable Aliphatic Polyesters. *Macromol. Biosci.* **2004**, *4*, 1075−1083.

(12) Ellis, A. V.; Chong, S.; Jansen, M. Formation of an α-Cyclodextrin/16-Mercaptohexadecanoic Acid Complex and Its Deposition on Gold Surfaces. *J. Inclusion Phenom. Macrocyclic Chem.* **2009**, *63*, 267−272.

(13) Raffaini, G.; Ganazzoli, F.; Malpezzi, L.; Fuganti, C.; Fronza, G.; Panzeri, W.; Mele, A. Validating a Strategy for Molecular Dynamics Simulations of Cyclodextrin Inclusion Complexes through Single-

Crystal X-Ray and NMR Experimental Data: A Case Study. *J. Phys. Chem. B* **2009**, *113*, 9110−9122.
(14) Saenger, W.; Noltemeyer, M.; Manor, P. C.; Hingerty, B.; Klar, B. "Induced-Fit"-Type Complex Formation of the Model Enzyme α-Cyclodextrin. *Bioorg. Chem.* **1976**, *5*, 187−195.
(15) Dodziuk, H. Rigidity Versus Flexibility. A Review of Experimental and Theoretical Studies Pertaining to the Cyclodextrin Nonrigidity. *J. Mol. Struct.* **2002**, *614*, 33−45.
(16) Zhang, H.; Ge, C.; van der Spoel, D.; Feng, W.; Tan, T. Insight into the Structural Deformations of β-Cyclodextrin Caused by Alcohol Cosolvents and Guest Molecules. *J. Phys. Chem. B* **2012**, *116*, 3880−3889.
(17) Zhang, H.; Feng, W.; Li, C.; Tan, T. Investigation of the Inclusions of Puerarin and Daidzin with β-Cyclodextrin by Molecular Dynamics Simulation. *J. Phys. Chem. B* **2010**, *114*, 4876−4883.
(18) Zheng, X.; Wang, D.; Shuai, Z.; Zhang, X. Molecular Dynamics Simulations of the Supramolecular Assembly between an Azobenzene-Containing Surfactant and α-Cyclodextrin: Role of Photoisomerization. *J. Phys. Chem. B* **2011**, *116*, 823−832.
(19) Pan, W.; Zhang, D.; Zhan, J. Theoretical Investigation on the Inclusion of Tcdd with β-Cyclodextrin by Performing Qm Calculations and Md Simulations. *J. Hazard. Mater.* **2011**, *192*, 1780−1786.
(20) Inoue, Y.; Hakushi, T.; Liu, Y.; Tong, L.; Shen, B.; Jin, D. Thermodynamics of Molecular Recognition by Cyclodextrins. 1. Calorimetric Titration of Inclusion Complexation of Naphthalenesulfonates with α-, β-, and γ-Cyclodextrins: Enthalpy−Entropy Compensation. *J. Am. Chem. Soc.* **1993**, *115*, 475−481.
(21) Rekharsky, M.; Inoue, Y. Chiral Recognition Thermodynamics of β-Cyclodextrin:The Thermodynamic Origin of Enantioselectivity and the Enthalpy−Entropy Compensation Effect. *J. Am. Chem. Soc.* **2000**, *122*, 4418−4435.
(22) Cai, W.; Sun, T.; Liu, P.; Chipot, C.; Shao, X. Inclusion Mechanism of Steroid Drugs into β-Cyclodextrins. Insights from Free Energy Calculations. *J. Phys. Chem. B* **2009**, *113*, 7836−7843.
(23) Dolenc, J.; Riniker, S.; Gaspari, R.; Daura, X.; van Gunsteren, W. Free Energy Calculations Offer Insights into the Influence of Receptor Flexibility on Ligand−Receptor Binding Affinities. *J. Comput. Aided Mol. Des.* **2011**, *25*, 709−716.
(24) Zhang, Q.; Tu, Y.; Tian, H.; Zhao, Y.-L.; Stoddart, J. F.; Ågren, H. Working Mechanism for a Redox Switchable Molecular Machine Based on Cyclodextrin: A Free Energy Profile Approach. *J. Phys. Chem. B* **2010**, *114*, 6561−6566.
(25) Sun, T.; Shao, X.; Cai, W. Self-Assembly Behavior of β-Cyclodextrin and Imipramine. A Free Energy Perturbation Study. *Chem. Phys.* **2010**, *371*, 84−90.
(26) Liu, P.; Cai, W.; Chipot, C.; Shao, X. Thermodynamic Insights into the Dynamic Switching of a Cyclodextrin in a Bistable Molecular Shuttle. *J. Phys. Chem. Lett.* **2010**, *1*, 1776−1780.
(27) El-Barghouthi, M. I.; Jaime, C.; Akielah, R. E.; Al-Sakhen, N. A.; Masoud, N. A.; Issa, A. A.; Badwan, A. A.; Zughul, M. B. Free Energy Perturbation and MM/PBSA Studies on Inclusion Complexes of Some Structurally Related Compounds with β-Cyclodextrin. *Supramol. Chem.* **2009**, *21*, 603−610.
(28) Keung, W. M.; Vallee, B. L. Kudzu Root: An Ancient Chinese Source of Modern Antidipsotropic Agents. *Phytochemistry* **1998**, *47*, 499−506.
(29) Lowe, E. D.; Gao, G.-Y.; Johnson, L. N.; Keung, W. M. Structure of Daidzin, a Naturally Occurring Anti-Alcohol-Addiction Agent, in Complex with Human Mitochondrial Aldehyde Dehydrogenase. *J. Med. Chem.* **2008**, *51*, 4482−4487.
(30) Moorwood, C.; Lozynska, O.; Suri, N.; Napper, A. D.; Diamond, S. L.; Khurana, T. S. Drug Discovery for Duchenne Muscular Dystrophy Via Utrophin Promoter Activation Screening. *Plos One* **2011**, *6*, e26169.
(31) Lemkul, J. A.; Bevan, D. R. Assessing the Stability of Alzheimer's Amyloid Protofibrils Using Molecular Dynamics. *J. Phys. Chem. B* **2010**, *114*, 1652−1660.
(32) Torrie, G. M.; Valleau, J. P. Nonphysical Sampling Distributions in Monte Carlo Free-Energy Estimation: Umbrella Sampling. *J. Comput. Phys.* **1977**, *23*, 187−199.
(33) Rashid, M. H.; Kuyucak, S. Affinity and Selectivity of Shk Toxin for the Kv1 Potassium Channels from Free Energy Simulations. *J. Phys. Chem. B* **2012**, *116*, 4812−4822.
(34) Hub, J. S.; Winkler, F. K.; Merrick, M.; de Groot, B. L. Potentials of Mean Force and Permeabilities for Carbon Dioxide, Ammonia, and Water Flux across a Rhesus Protein Channel and Lipid Membranes. *J. Am. Chem. Soc.* **2010**, *132*, 13251−13263.
(35) Wennberg, C. L.; van der Spoel, D.; Hub, J. S. Large Influence of Cholesterol on Solute Partitioning into Lipid Membranes. *J. Am. Chem. Soc.* **2012**, *134*, 5351−5361.
(36) Caleman, C.; Hub, J. S.; van Maaren, P. J.; van der Spoel, D. Atomistic Simulation of Ion Solvation in Water Explains Surface Preference of Halides. *Proc. Natl. Acad. Sci.* **2011**, *108*, 6838−6842.
(37) Hub, J. S.; Caleman, C.; van der Spoel, D. Organic Molecules on the Surface of Water Droplets—An Energetic Perspective. *Phys. Chem. Chem. Phys.* **2012**, *14*, 9537−9545.
(38) Cezard, C.; Trivelli, X.; Aubry, F.; Djedaini-Pilard, F.; Dupradeau, F. Y. Molecular Dynamics Studies of Native and Substituted Cyclodextrins in Different Media: 1. Charge Derivation and Force Field Performances. *Phys. Chem. Chem. Phys.* **2011**, *13*, 15103−15121.
(39) Zhang, H.; Tan, T.; Feng, W.; van der Spoel, D. Molecular Recognition in Different Environments: β-Cyclodextrin Dimer Formation in Organic Solvents. *J. Phys. Chem. B* **2012**, *116*, 12684−12693.
(40) Hess, B.; Kutzner, C.; van der Spoel, D.; Lindahl, E. GROMACS 4: Algorithms for Highly Efficient, Load-Balanced, and Scalable Molecular Simulation. *J. Chem. Theory Comput.* **2008**, *4*, 435−447.
(41) van der Spoel, D.; Lindahl, E.; Hess, B.; Groenhof, G.; Mark, A. E.; Berendsen, H. J. C. GROMACS: Fast, Flexible, and Free. *J. Comput. Chem.* **2005**, *26*, 1701−1718.
(42) Wang, J. M.; Wolf, R. M.; Caldwell, J. W.; Kollman, P. A.; Case, D. A. Development and Testing of a General Amber Force Field. *J. Comput. Chem.* **2004**, *25*, 1157−1174.
(43) Besler, B. H.; Merz, K. M.; Kollman, P. A. Atomic Charges Derived from Semiempirical Methods. *J. Comput. Chem.* **1990**, *11*, 431−439.
(44) Frisch, M. J., Trucks, G. W., Schlegel, H. B., Scuseria, G., Scuseria, E., Robb, M. A., Cheeseman, J. R., Montgomery, J. A., Vreven, T., Kudin, K. N., Burant, J. C., Millam, J. M., Iyengar, S. S., Tomasi, J., Barone, V., Mennucci, B., Cossi, M., Scalmani, G., Rega, N., Petersson, G. A., Nakatsuji, H., Hada, M., Ehara, M., Toyota, K., Fukuda, R., Hasegawa, J., Ishida, M., Nakajima, T., Honda, Y., Kitao, O., Nakai, H., Klene, M., Li, X., Knox, J. E., Hratchian, H. P., Cross, J. B., Bakken, V., Adamo, C., Jaramillo, J., Gomperts, R., Stratmann, R. E., Yazyev, O., Austin, A. J., Cammi, R., Pomelli, C., Ochterski, J. W., Ayala, P. Y., Morokuma, K., Voth, G. A., Salvador, P., Dannenberg, J. J., Zakrzewski, V. G., Dapprich, S., Daniels, A. D., Strain, M. C., Farkas, O., Malick, D. K., Rabuck, A. D., Raghavachari, K., Foresman, J. B., Ortiz, J. V., Cui, Q., Baboul, A. G., Clifford, S., Cioslowski, J., Stefanov, B. B., Liu, G., Liashenko, A., Piskorz, P., Komaromi, I., Martin, R. L., Fox, D. J., Keith, T., Al-Laham, M. A., Peng, C. Y., Nanayakkara, A., Challacombe, M., Gill, P. M. W., Johnson, B., Chen, W., Wong, M. W., Gonzalez, C., Pople, J. A. *Gaussian 03*, Revision C.02; Gaussian, Inc.: Wallingford, CT, 2004.
(45) Hess, B.; Bekker, H.; Berendsen, H. J. C.; Fraaije, J. G. E. M. Lincs: A Linear Constraint Solver for Molecular Simulations. *J. Comput. Chem.* **1997**, *18*, 1463−1472.
(46) Miyamoto, S.; Kollman, P. A. Settle—An Analytical Version of the Shake and Rattle Algorithm for Rigid Water Models. *J. Comput. Chem.* **1992**, *13*, 952−962.
(47) Jorgensen, W. L.; Chandrasekhar, J.; Madura, J. D.; Impey, R. W.; Klein, M. L. Comparison of Simple Potential Functions for Simulating Liquid Water. *J. Chem. Phys.* **1983**, *79*, 926−935.

(48) Essmann, U.; Perera, L.; Berkowitz, M. L.; Darden, T.; Lee, H.; Pedersen, L. G. A Smooth Particle Mesh Ewald Method. *J. Chem. Phys.* **1995**, *103*, 8577−8593.
(49) Darden, T.; York, D.; Pedersen, L. Particle Mesh Ewald—An N.Log(N) Method for Ewald Sums in Large Systems. *J. Chem. Phys.* **1993**, *98*, 10089−10092.
(50) Parrinello, M.; Rahman, A. Polymorphic Transitions in Single Crystals: A New Molecular Dynamics Method. *J. Appl. Phys.* **1981**, *52*, 7182−7190.
(51) Kumar, S.; Rosenberg, J. M.; Bouzida, D.; Swendsen, R. H.; Kollman, P. A. The Weighted Histogram Analysis Method for Free-Energy Calculations on Biomolecules. I. The Method. *J. Comput. Chem.* **1992**, *13*, 1011−1021.
(52) Hub, J. S.; de Groot, B. L.; van der Spoel, D. g_wham—A Free Weighted Histogram Analysis Implementation Including Robust Error and Autocorrelation Estimates. *J. Chem. Theory Comput.* **2010**, *6*, 3713−3720.
(53) Hess, B. Determining the Shear Viscosity of Model Liquids from Molecular Dynamics Simulations. *J. Chem. Phys.* **2002**, *116*, 209−217.
(54) Andricioaei, I.; Karplus, M. On the Calculation of Entropy from Covariance Matrices of the Atomic Fluctuations. *J. Chem. Phys.* **2001**, *115*, 6289−6292.
(55) Zhao, R.; Tan, T.; Sandström, C. NMR Studies on Puerarin and Its Interaction with β-Cyclodextrin. *J. Biol. Phys.* **2011**, *37*, 387−400.
(56) Valero, M.; Costa, S. M. B.; Ascenso, J. R.; Mercedes Velázquez, M.; Rodríguez, L. J. Complexation of the Non-Steroidal Anti-Inflammatory Drug Nabumetone with Modified and Unmodified Cyclodextrins. *J. Inclusion Phenom. Macrocyclic Chem.* **1999**, *35*, 663−677.
(57) Zhang, H.; Feng, W.; Li, C.; Lv, Y.; Tan, T. A Model for the Shuttle Motions of Puerarin and Daidzin inside the Cavity of β-Cyclodextrin in Aqueous Acetic Acid: Insights from Molecular Dynamics Simulations. *J. Mol. Model.* **2012**, *18*, 221−227.
(58) Auletta, T.; de Jong, M. R.; Mulder, A.; van Veggel, F. C. J. M.; Huskens, J.; Reinhoudt, D. N.; Zou, S.; Zapotoczny, S.; Schönherr, H.; Vancso, G. J.; Kuipers, L. β-Cyclodextrin Host−Guest Complexes Probed under Thermodynamic Equilibrium: Thermodynamics and AFM Force Spectroscopy. *J. Am. Chem. Soc.* **2004**, *126*, 1577−1584.
(59) Yu, Y.; Chipot, C.; Cai, W.; Shao, X. Molecular Dynamics Study of the Inclusion of Cholesterol into Cyclodextrins. *J. Phys. Chem. B* **2006**, *110*, 6372−6378.
(60) Filippini, G.; Goujon, F.; Bonal, C.; Malfreyt, P. Energetic Competition Effects on Thermodynamic Properties of Association between β-CD and Fc Group: A Potential of Mean Force Approach. *J. Phys. Chem. C* **2012**, *116*, 22350−22358.
(61) Deng, Y.; Roux, B. Calculation of Standard Binding Free Energies: Aromatic Molecules in the T4 Lysozyme L99a Mutant. *J. Chem. Theory Comput.* **2006**, *2*, 1255−1273.
(62) Borghetti, G. S.; Pinto, A. P.; Lula, I. S.; Sinisterra, R. D.; Teixeira, H. F.; Bassani, V. L. Daidzein/Cyclodextrin/Hydrophilic Polymer Ternary Systems. *Drug Dev. Ind. Pharm.* **2011**, *37*, 886−893.
(63) Todorova, N. A.; Schwarz, F. P. The Role of Water in the Thermodynamics of Drug Binding to Cyclodextrin. *J. Chem. Thermodyn.* **2007**, *39*, 1038−1048.
(64) Goyenechea, N.; Sánchez, M.; Vélaz, I.; Martín, C.; Martínez-Ohárriz, M. C.; González-Gaitano, G. Inclusion Complexes of Nabumetone with β-Cyclodextrins: Thermodynamics and Molecular Modelling Studies. Influence of Sodium Perchlorate. *Luminescence* **2001**, *16*, 117−127.
(65) Brocos, P.; Díaz-Vergara, N.; Banquy, X.; Pérez-Casas, S.; Costas, M.; Piñeiro, A. n. Similarities and Differences between Cyclodextrin−Sodium Dodecyl Sulfate Host−Guest Complexes of Different Stoichiometries: Molecular Dynamics Simulations at Several Temperatures. *J. Phys. Chem. B* **2010**, *114*, 12455−12467.
(66) Ishizu, T.; Kintsu, K.; Yamamoto, H. NMR Study of the Solution Structures of the Inclusion Complexes of β-Cyclodextrin with (+)-Catechin and (−)-Epicatechin. *J. Phys. Chem. B* **1999**, *103*, 8992−8997.
(67) Yan, C.; Xiu, Z.; Li, X.; Hao, C. Molecular Modeling Study of β-Cyclodextrin Complexes with (+)-Catechin and (−)-Epicatechin. *J. Mol. Graphics Modell.* **2007**, *26*, 420−428.
(68) Zifferer, G.; Sellner, B.; Kornherr, A.; Krois, D.; Brinker, U. H. Molecular Dynamics Simulations of β-Cyclodextrin-Aziadamantane Complexes in Water. *J. Phys. Chem. B* **2008**, *112*, 710−714.
(69) He, J.; Chipot, C.; Shao, X.; Cai, W. Cyclodextrin-Mediated Recruitment and Delivery of Amphotericin B. *J. Phys. Chem. C* **2013**, *117*, 11750−11756.
(70) Liu, P.; Chipot, C.; Shao, X.; Cai, W. How Do α-Cyclodextrins Self-Organize on a Polymer Chain? *J. Phys. Chem. C* **2012**, *116*, 17913−17918.
(71) Liu, P.; Chipot, C.; Shao, X.; Cai, W. Solvent-Controlled Shuttling in a Molecular Switch. *J. Phys. Chem. C* **2012**, *116*, 4471−4476.
(72) Lopez, C. A.; de Vries, A. H.; Marrink, S. J. Computational Microscopy of Cyclodextrin Mediated Cholesterol Extraction from Lipid Model Membranes. *Sci. Rep.* **2013**, *3*, 2071.
(73) Yamazaki, T.; Kovalenko, A. Spatial Decomposition Analysis of the Thermodynamics of Cyclodextrin Complexation. *J. Chem. Theory Comput.* **2009**, *5*, 1723−1730.
(74) Wickstrom, L.; He, P.; Gallicchio, E.; Levy, R. M. Large Scale Affinity Calculations of Cyclodextrin Host−Guest Complexes: Understanding the Role of Reorganization in the Molecular Recognition Process. *J. Chem. Theory Comput.* **2013**, *9*, 3136−3150.
(75) Southall, N. T.; Dill, K. A.; Haymet, A. D. J. A View of the Hydrophobic Effect. *J. Phys. Chem. B* **2001**, *106*, 521−533.
(76) Chandler, D. Interfaces and the Driving Force of Hydrophobic Assembly. *Nature* **2005**, *437*, 640−647.
(77) Jorgensen, W. L. Efficient Drug Lead Discovery and Optimization. *Acc. Chem. Res.* **2009**, *42*, 724−733.
(78) Schneider, G. Virtual Screening: An Endless Staircase? *Nat. Rev. Drug Discov.* **2010**, *9*, 273−276.
(79) Hetényi, C.; van der Spoel, D. Toward Prediction of Functional Protein Pockets Using Blind Docking and Pocket Search Algorithms. *Protein Sci.* **2011**, *20*, 880−893.
(80) Carlsson, J.; Boukharta, L.; Åqvist, J. Combining Docking, Molecular Dynamics and the Linear Interaction Energy Method to Predict Binding Modes and Affinities for Non-Nucleoside Inhibitors to HIV-1 Reverse Transcriptase. *J. Med. Chem.* **2008**, *51*, 2648−2656.
(81) Warren, G. L.; Andrews, C. W.; Capelli, A.-M.; Clarke, B.; LaLonde, J.; Lambert, M. H.; Lindvall, M.; Nevins, N.; Semus, S. F.; Senger, S.; Tedesco, G.; Wall, I. D.; Woolven, J. M.; Peishoff, C. E.; Head, M. S. A Critical Assessment of Docking Programs and Scoring Functions. *J. Med. Chem.* **2005**, *49*, 5912−5931.
(82) Zhou, H. X.; Gilson, M. K. Theory of Free Energy and Entropy in Noncovalent Binding. *Chem. Rev.* **2009**, *109*, 4092−4107.
(83) Schlitter, J. Estimation of Absolute and Relative Entropies of Macromolecules Using the Covariance Matrix. *Chem. Phys. Lett.* **1993**, *215*, 617−621.
(84) Carlsson, J.; Åqvist, J. Absolute and Relative Entropies from Computer Simulation with Applications to Ligand Binding. *J. Phys. Chem. B* **2005**, *109*, 6448−6456.
(85) Chen, W.; Chang, C.-E.; Gilson, M. K. Calculation of Cyclodextrin Binding Affinities: Energy, Entropy, and Implications for Drug Design. *Biophys. J.* **2004**, *87*, 3035−3049.